View metadata, citation and similar papers at core.ac.uk

brought to you by CORE

provided by Elsevier - Publisher Connector

ASIAN JOURNAL OF PHARMACEUTICAL SCIENCES 9 (2014) 324–329

HOSTED BY

ELSEVIER

Available online at www.sciencedirect.com

ScienceDirect

journal homepage: http://ees.elsevier.com/ajps/default.asp

Original Research Paper

Effect of the glyceryl monooleate-based lyotropic phases on skin permeation using *in vitro* diffusion and skin imaging

Dae Gon Lim [a], *Won-Wook Jeong* [b], *Nam Ah Kim* [a], *Jun Yeul Lim* [a], *Seol-Hoon Lee* [b], *Woo Sun Shim* [b], *Nae-Gyu Kang* [b,**], *Seong Hoon Jeong* [a,*]

[a] *College of Pharmacy, Dongguk University-Seoul, Goyang, Gyeonggi 410-820, Republic of Korea*

[b] *LG Household & Health Care, Daejeon 305-343, Republic of Korea*

ARTICLE INFO

Article history:
Received 28 March 2014
Received in revised form
18 June 2014
Accepted 19 June 2014
Available online 27 August 2014

Keywords:
Confocal microscopy
Imaging
Glyceryl monooleate
Skin permeation
Cubic phase
Lamellar phase

ABSTRACT

Glyceryl monooleate (GMO) is a polar lipid that can exist in various liquid crystalline phases in the presence of different amounts of water. It is regarded as a permeation enhancer due to its amphiphilic property. Various phases of GMO/solvent system containing sodium fluorescein were prepared to compare permeability using confocal laser scanning microscopy (CLSM). GMO was melted in a vial in a water bath heated to 45 °C. Propylene glycol and hexanediol were homogeneously dissolved in the melted GMO. Sodium fluorescein in aqueous solution was diluted to various ratios and thoroughly mixed by an ultrasonic homogenizer. Each GMO/Solvent system with fluorescein was applied onto the epidermal side of excised pig skin and incubated overnight. CLSM was performed to observe how the GMO/solvent system in its different phases affect skin permeability. Cubic and lamellar phase formulations enhanced the fluorescein permeation through the stratum corneum. A solution system had the weakest permeability compared to the other two phases. Due to the amphiphilic nature of GMO, cubic and lamellar phases might reduce the barrier function of stratum corneum which was observed by CLSM as fluorescein accumulated in the dermis. Based on the results, the glyceryl monooleate lyotropic mixtures could be applied to enhance skin permeation in various topical and transdermal formulations.

© 2014 Shenyang Pharmaceutical University. Production and hosting by Elsevier B.V. All rights reserved.

1. Introduction

Glyceryl monooleate (GMO) is a well-known molecule commonly used as an emulsifying agent, biocompatible controlled-release material, and a food additive. It is considered as a nontoxic, biodegradable, and biocompatible material classified as "generally recognized as safe" (GRAS). It is included in the FDA Inactive Ingredients Guide and present in nonparenteral medicines in the United Kingdom [1].

* *Corresponding author.*
** *Corresponding author.*
E-mail addresses: ngkang@lgcare.com (N.-G. Kang), shjeong@dongguk.edu (S.H. Jeong).
Peer review under responsibility of Shenyang Pharmaceutical University.
http://dx.doi.org/10.1016/j.ajps.2014.06.008
1818-0876/© 2014 Shenyang Pharmaceutical University. Production and hosting by Elsevier B.V. All rights reserved.

GMO is a polar lipid with the ability to form various liquid crystalline phases in the presence of different amounts of water. In the presence of a small amount of water, GMO forms reversed micelles characterized by an oily texture. As more water is added, a mucous-like system is formed that corresponds to the lamellar phase. A large isotropic phase region dominates when more water is added (20 ~ 40%). This phase, known as the cubic phase, is highly viscous. In addition, the temperature and ratio of weight to water plays a role in the various phases of GMO. In the presence of high amounts of water in temperatures ranging from 20 ~ 70 °C, the cubic phase might exist in a stable condition [2]. The cubic phase is said to be bicontinuous since it consists of a curved bilayer extending in three dimensions, separating two congruent water channel networks. The water pore diameter is about 5 nm when the cubic phase is fully swollen. The presence of a lipid and an aqueous domain gives special properties to the cubic phase such as the ability to solubilize hydrophilic, hydrophobic, and amphiphilic substances [3].

Previous research has demonstrated that the liquid crystalline phases of GMO such as the cubic and reversed hexagonal phase, increased transdermal drug delivery [4]. The advantages of the formulations for transdermal drug delivery system might include biocompatibility and the ability to self-assemble their structure. The cubic phase of GMO can be dispersed in a water-rich environment and form a dispersion containing nanometer-sized particles. GMO's interaction with phospholipid bilayers might suggest why it is known as a permeation enhancer [5].

In the current study, effects of various formulations of GMO/water system on skin permeability were evaluated using Franz-diffusion cells and confocal laser scanning microscopy (CLSM). To test the permeability of each formulation, sodium fluorescein was added to the mixture that was applied on excised pig skin. Even though the influence of GMO on the percutaneous absorption through hairless mouse skin has been studied [6], differences between the GMO/water formulations and how they affect permeability and distribution throughout the layers of the skin have not been investigated. This study might provide an insight to understand the effects of formulation on the skin permeation.

2. Material and methods

2.1. Materials

Glyceryl monooleate (GMO), propylene glycol, hexanediol, paraformaldehyde, sodium chloride, potassium chloride, potassium phosphate monobasic, potassium phosphate dibasic, and sodium fluorescein were purchased from Sigma–Aldrich Co. (St. Louis, MO, USA). Excised pig skin obtained from PWG Genetics Korea, Ltd. (Pyeongtaek, Gyeonggi, Korea). FSC 22 Frozen section media was purchased from Leica Biosystems (Wetzlar, Hesse, Germany). Hydrophobic PTFE membrane was purchased from Pall Corporation (New York, NY, USA). Hydrophilic nitrocellulose membrane was purchased from EMD Millipore (Billerica, MA, USA).

2.2. Preparation of formulations

Three different formulations were prepared for the current study (Table 1). Lyotropic liquid crystalline phases (cubic and lamellar phases) were produced by melting GMO in a vial at 45 °C and then propylene glycol and hexanediol were dissolved in the melted GMO. Propylene glycol was utilized in order to slow down the drastic increase of viscosity during the cubic phase formation by mixing GMO and water. A small amount of hexanediol was added to prevent bacterial growth in the mixture and prolong the shelf-life. An aqueous solution of fluorescein was produced by dissolving hexanediol and sodium fluorescein in deionized water. The aqueous solution of sodium fluorescein was slowly added to the mixture while it was strongly agitated by an ultrasonic homogenizer to form lyotropic liquid crystalline phases.

2.3. In vitro diffusion studies with membranes

In vitro diffusion study was carried out using Franz-type diffusion cells assembled with hydrophobic PTFE membrane and hydrophilic nitrocellulose membrane between the donor and receptor chambers. The volume of each chamber was 12.5 ml and the diffusion area was 1.82 cm^2. Pore size of the membranes was 0.45 μm. To simulate a skin's lipid-bilayer, hydrophobic membranes were dipped in melted GMO and soaked in receptor medium for 30 min before diffusion studies. After the membranes were soaked, the hydrophobic membrane was attached to the hydrophilic membrane and both remained attached during the diffusion experiment.

The receptor chamber was filled with phosphate buffered saline (pH 7.4). The donor chamber containing the cubic phase, lamellar phase, or solution samples with 1 mg/ml of the sodium fluorescein were applied on the upper surface of the hydrophobic membrane. Receptor components were continuously stirred with a magnetic stirrer and samples were withdrawn at predetermined time intervals (1, 2, 3, 4, 6, 8, and 12 h). After withdrawing samples from the receptor, the receptor was replaced with the same volume of fresh phosphate buffered saline to maintain sink condition. The content of sodium fluorescein was analyzed by multi-mode microplate reader. The cumulative amount of sodium fluorescein released per surface area was obtained using the following equation:

$$Q = \left\{ C_n V + \sum_{i=1}^{n-1} C_i S \right\} \Big/ A$$

where Q is the cumulative amounts of sodium fluorescein released per surface area of the membrane (μg/cm^2) and Cn

Table 1 – Compositions of cubic, lamellar, and solution formulations for the current study.

Component	Cubic phase	Lamellar phase	Solution
Water	0.199	0.119	0.969
Glyceryl monooleate	0.650	0.850	–
Propylene glycol	0.120	–	–
Hexanediol	0.030	0.030	0.030
Sodium fluorescein	0.001	0.001	0.001

is the concentration of the sodium fluorescein (μg/ml) determined at *n*th sampling interval. *V* is the volume of individual Franz-type diffusion cell, *S* is the volume of sampling aliquot (0.5 ml), and *A* is the surface area of membrane. The cumulative amounts released per surface area were plotted against time. The steady-state flux (*J*) was obtained from the slope of the linear portion of plotted cumulative released amounts of compound. The lag time (T_{lag}) was obtained from the intercept of extrapolated linear portion with time axis (*x*-axis). Statistical analysis was performed using the student's *t* test and analysis variance (one-way ANOVA, Dunnett's multiple comparison test of SigmaStat 3.5, Dundas software, Germany) with a *P*-value of ≤ 0.05 considered to be significant.

2.4. *Fluorescence assay*

Fluorescence emission spectra of sodium fluorescein were obtained using SpectraMax M3 multi-mode microplate reader (Molecular device, Sunnyvale, CA, USA). Excitation wavelength was 492 nm and emission wavelength was 515 nm with a 4 nm silt width. The spectra of samples were corrected by subtracting the corresponding buffer spectra. Before obtaining the fluorescence of diffused sodium fluorescein, linearity of the calibration curve was obtained by plotting the nominal concentration of the standard sodium fluorescein (x) versus the emission spectra intensity (y) in the tested concentration range. Accuracy and precision were determined by analyzing samples in triplicate six times on the same day.

2.5. *Confocal laser scanning microscopy (CLSM)*

Cubic, lamellar, and solution formulations containing 1 mg/ml of the fluorescein were applied onto the pig skin and left for 5 h and 24 h at 37 °C. After the treatment, skin samples were fixed with 4% paraformaldehyde for 24 h. The fixed skin samples were embedded in frozen section media and frozen overnight in a deep freezer at −82.7 °C. The frozen skin samples were cross-sectioned into slices 20 μm thick by Leica CM1520 cryostat for cell nuclei staining. Sections were stained with 1 μg/ml of 4′, 6-diamidino-2-phenylindole (DAPI) for 10 min at 37 °C. After washing with PBS, the cross-section of the skin samples were imaged by LSM 510 microscope (Carl Zeiss AG, Oberkochen, Baden-Württemberg, Germany) with dual excitation band of DAPI (358 nm) and FITC filter (488 nm). Fluorescence imaging processing was performed by ZEN 2012 software and Adobe Photoshop.

3. Result and discussion

3.1. *In vitro diffusion studies with membranes*

To validate the fluorescence assay method, calibration curves of the sodium fluorescein were plotted and found to be linear ($R^2 \geq 0.999$) in the tested range of 0.064–32 μg/ml (Table 2). The limit of detection (LOD) and limit of quantification (LOQ) were 0.015 and 0.046 μg/ml, respectively. The accuracy for 0.32, 1.6, and 32 mg/ml sodium fluorescein standard solutions ($n = 3$) was 2.25, 1.77, and 0.28, respectively (expressed as % variation of the mean). The precision for 0.32, 1.6, and 32 mg/ml sodium fluorescein standard solutions ($n = 3$) was 3.03, 2.32, and 0.19, respectively (expressed as % coefficient of variation).

Table 2 – Properties of the sodium fluorescein calibration curves using confocal microscopy.

Number	Range (μg/ml)	Slope	Intercept	R^2
1	0.064–32	1702.7617	74.4438	0.9996
2		1690.0246	62.9946	0.9995
3		1696.3530	78.0563	0.9998
Average		1696.3797	71.8316	0.9997
SD		6.3686	7.8633	0.0001
RSD (%)		0.3754	10.9468	0.0109

The diffusion profiles of sodium fluorescein in various formulations across the synthetic membrane are shown in Fig. 1. As the cumulative amount of sodium fluorescein released per unit surface area in the receptor phase was plotted against time, a linear relationships after a lag time was obtained. The diffusion coefficient and flux of each formulation were calculated from the slope and lag time (Table 3). Flux of sodium fluorescein across the synthetic membrane in descending order was the cubic phase (15.11 μg/cm^2 h), lamellar phase (12.45 μg/cm^2 h), and solution formulation (8.23 μg/cm^2 h). The cumulative amount of sodium fluorescein released at 12 h and fluxes of the cubic and lamellar phases were significantly greater ($P < 0.05$) than those of the solution formulation. The cubic and lamellar phases released about 80 and 39 times more, respectively, compared to the solution. Since sodium fluorescein is hydrophilic and water-soluble, diffusion through an oil-wetted hydrophobic membrane may be a limiting factor. Differences in lag time and flux might cause significant differences in the amount of sodium fluorescein released between each GMO/water formulations. In addition, the hydrophobicity of GMO in each formulation may have an effect on the sodium fluorescein's permeability through oil-wetted hydrophobic membrane. In a study investigating the effect of permeation enhancers on transdermal delivery, GMO increased the flux across skin for both hydrophilic and hydrophobic drugs by inducing reversible

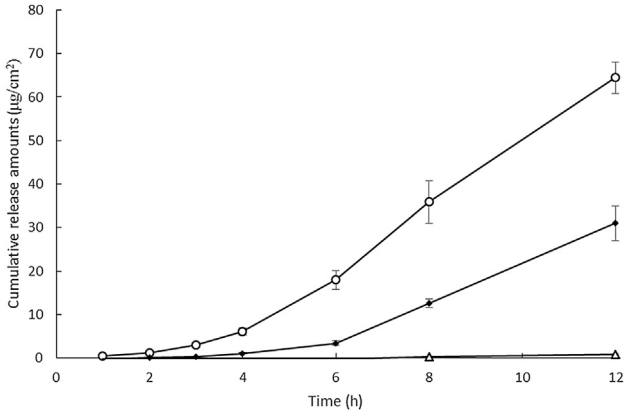

Fig. 1 – *In vitro* analysis of sodium fluorescein release (μg/cm^2) across the synthetic membrane from (○) cubic phase, (●) lamellar phase, and (Δ) solution ($n = 3$).

Table 3 – *In vitro* release profiles of the sodium fluorescein across the synthetic membrane using different formulations ($n = 3$).

Formulation	Flux ($\mu g/cm^2\ h^{-1}$)	Diffusion coefficient (mm^2/h)	Lag time (h)	Cumulative release amounts after 12 h ($\mu g/cm^2$)
Cubic phase	15.11 ± 1.30	0.00453 ± 0.00039	3.31 ± 0.33	64.47 ± 3.60
Lamellar phase	11.02 ± 0.37	0.00331 ± 0.00011	4.53 ± 0.15	30.99 ± 3.95
Solution	8.23 ± 0.28	0.00247 ± 0.00008	6.08 ± 0.24	0.80 ± 0.14

disruption of the lamellar structure of the lipid bilayer and increasing the fluidity of lipids in skin [7].

Even though the lamellar phase has more GMO than the cubic phase formulation, the cubic phase released a higher cumulative amount of sodium fluorescein. A reasonable explanation for this is that propylene glycol enhanced the release of sodium fluorescein in the cubic phase formulation by reducing its viscosity which increased membrane permeability. The lamellar phase shifted to the cubic phase as water content increasing during membrane permeation [8]. The shift to cubic phase may have increased the viscosity and therefore decreased its mobility. It is likely that excess amounts of GMO might disturb diffusion through a membrane in lamellar phase. In the presence of propylene glycol, GMO also forms a liquid sponge phase which has a bicontinuous lipid water system [9]. Previous research has demonstrated that the liquid sponge phase had a better diffusion profile than the cubic phase formulation. Even though cubic phase formulation might not form the liquid sponge phase during diffusion in these experiments, an interaction between GMO and propylene glycol could promote diffusion through the membranes. Hydration time might be a factor in the difference in the diffusion rates between the different formulations. A previous study found that samples hydrated prior to the experiments released large amounts of drug because hydrophilic channels were available during the release of the drug [10]. As the initial water content increased, drug release increased due to the increased hydrophilic domain which accounted for the difference in the amount of drug initially released [11].

3.2. *Confocal microscopy imaging*

CLSM was used to observe the distribution of fluorescein in the skin layers after the application of cubic, lamellar, and solution formulation. Microscopic images of cross-sections perpendicular to the skin allowed us to observe the distribution pattern of the fluorescein in the deep region of the excised skin including the stratum corneum (SC), viable epidermis, and dermis. The diffusion profiles of sodium fluorescein into the skin was compared after the application of the different formulations. As shown in Fig. 2, the distribution of sodium fluorescein in the skin was visualized by CLSM after 5 h of topical application.

GMO might facilitate the diffusion of sodium fluorescein through the viable epidermis and dermis. The cubic phase was uniformly distributed in the epidermis and dermis (Fig. 2A). The lamellar phase also showed relatively uniform distribution in epidermis and dermis with a small amount present in the SC (Fig. 2B). Most of the sodium fluorescein in the solution formulation was unable to permeate the SC region (Fig. 2C). The image of skin that had the solution formulation applied to it showed a relatively low intensity of fluorescence at the epidermis and dermal layer, but a very strong intensity on the SC. These results support the previous results of diffusion experiment using Franz-type diffusion cells that looked at flux, lag time, and diffusion coefficient between different formulations.

Fig. 3 shows the confocal images of the skin after 24 h of sample application. The cubic and lamellar phase formulations showed much stronger fluorescence in the dermal layer compared to the solution formulation. Cubic and lamellar phases showed strong fluorescence in the dermis after 24 h of application compared to 5 h-images. Solution formulation also showed stronger fluorescence than its 5 h-image, but it was localized in the SC layer. This result might suggest that most of sodium fluorescein in the solution formulation might not be able to penetrate SC layer. However, with its low molecular weight sodium fluorescein might be distributed to the SC region which could not be removed during washing, and still showed localized fluorescence after 24 h (Fig. 3C).

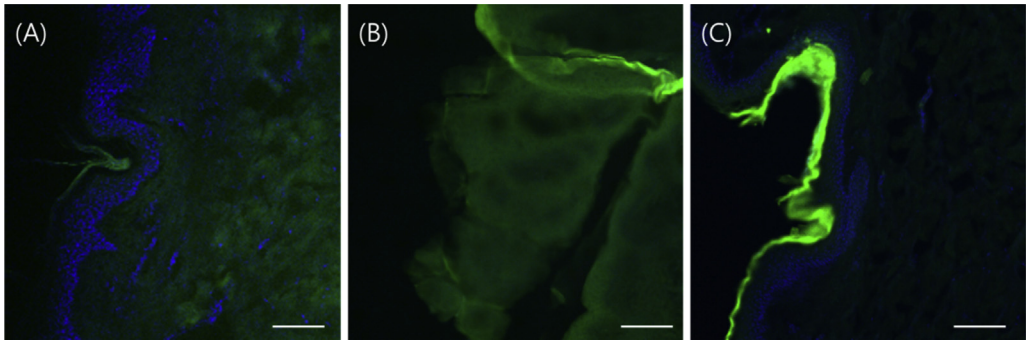

Fig. 2 – CLSM images to evaluate the distribution of the sodium fluorescein in excised pig skin after 5 h of sample application: (A) cubic phase, (B) lamellar phase, and (C) solution formulation. Each scale bar indicates 100 μm.

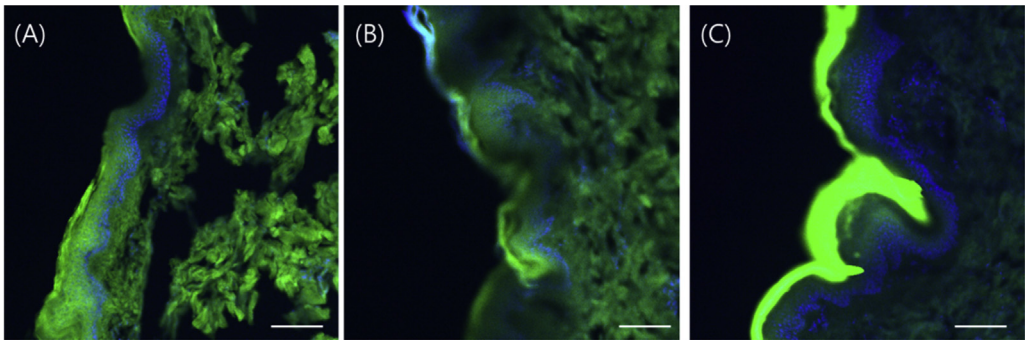

Fig. 3 – CLSM images to evaluate the distribution of the sodium fluorescein in excised pig skin after 24 h of sample application: (A) cubic phase, (B) lamellar phase, and (C) solution formulation. Each scale bar indicates 100 μm.

During a skin diffusion test, GMO might reversibly emulsify the lipid matrix of the skin and penetrate through the SC [12]. Because adipose tissue and the hypodermis are more hydrophobic than other tissues they make up the skin, most GMO formulations might interact with the tissues and accumulate in them. Therefore, confocal images of samples treated with the cubic and lamellar phases showed stronger fluorescence at hypodermis and adipose tissues than other tissues in skin. In addition, the cubic and lamellar phases showed some localization of high intensity fluorescence in dermis and adipose tissues. The solution formulation showed no localization in the tissues. Differences in localization might be caused by the presence of GMO in formulation. Lipids such as oleic acid and GMO have a polar head and a relatively short hydrophobic carbon chain that increases membrane permeability by promoting disorder of intercellular lipids [13]. In this study, intercellular lipid disorder might cause localization of the sodium fluorescein in the dermis and adipose tissue. Different absorption pathways might also cause difference in the amount of sodium fluorescein diffused between each formulation. Intercellular pathway seems to be predominant method of transdermal absorption when using the solution formulation, whereas the intercluster pathway is the most common method of absorption for the cubic and lamellar phase formulations [14]. Higher GMO concentrations did not improve permeability. The intensity of the fluorescence in the dermis was directly correlated with an increased with the permeability and not GMO concentration. At 37 °C, GMO might exist in a cubic phase when the amount of water is greater than 40% [15]. During the diffusion test, the lamellar phase might be hydrated by moisture in the skin and converted to cubic phase. Therefore, viscosity may increase, which decreases the mobility of the GMO/solvent mixture.

4. Conclusion

This study suggests that GMO is feasible as an absorption enhancer for topical drugs. Franz-type diffusion test and CLSM images in excised pig skin showed improved permeability through the hydrophobic-hydrophilic membrane and excised pig skin. Both cubic and lamellar formulations with GMO showed higher permeability and diffusion profiles. By comparing the diffusion patterns and confocal images, the cubic phase performed significantly better than the lamellar formulation. The results suggest that differences of diffusion were caused by ability of the GMO/solvent mixture to induce lipid disorder in the skin samples. These results support the hypothesis that GMO induces intercellular lipid disorder. High GMO/water ratio does not correlate with high membrane permeability. The cubic phase contained lower GMO concentration compared to the lamellar phase but had better membrane permeability. Our study demonstrates that GMO is an important substance for SC permeation but the viscosity of this formulation needs to be further investigated to improve the diffusion efficacy of active ingredients.

Acknowledgments

This study was supported by Basic Science Research Program through the National Research Foundation of Korea (NRF) funded by the Korean Ministry of Education, Science and Technology (2012002399) and a grant of the Korean Healthcare Technology R&D Project, Ministry of Health and Welfare, Republic of Korea. (Grant No.: A103017).

REFERENCES

[1] Ganem-Quintanar A, Quintanar-Guerrero D, Buri P. Monoolein: a review of the pharmaceutical applications. Drug Dev Ind Pharm 2000;26:809–820.
[2] Sallam A-S, Khalil E, Ibrahim H, et al. Formulation of an oral dosage form utilizing the properties of cubic liquid crystalline phases of glyceryl monooleate. Eur J Pharm Biopharm 2002;53:343–352.
[3] Lindblom G, Rilfors L. Cubic phases and isotropic structures formed by membrane lipids—possible biological relevance. Biochim Biophys Acta (BBA)-Rev Biomembr 1989;988:221–256.
[4] Lopes LB, Speretta FF, Bentley M. Enhancement of skin penetration of vitamin K using monoolein-based liquid crystalline systems. Eur J Pharm Sci 2007;32:209–215.
[5] Ferreira DA, Bentley MVL, Karlsson G, et al. Cryo-TEM investigation of phase behaviour and aggregate structure in

dilute dispersions of monoolein and oleic acid. Int J Pharm 2006;310:203–212.
[6] Pereira GR, Collett JH, Garcia SB, et al. Glycerol monooleate/solvents systems for progesterone transdermal delivery: in vitro permeation and microscopic studies. Rev Bras Cienc Farm 2002;38:55–62.
[7] Giannakou S, Dallas P, Rekkas D, et al. Development and in vitro evaluation of nitrendipine transdermal formulations using experimental design techniques. Int J Pharm 1995;125:7–15.
[8] Nesseem DI. Formulation and evaluation of itraconazole via liquid crystal for topical delivery system. J Pharm Biomed 2001;26:387–399.
[9] Alfons K, Engstrom S. Drug compatibility with the sponge phases formed in monoolein, water, and propylene glycol or poly (ethylene glycol). J Pharm Sci 1998;87:1527–1530.
[10] Lee J, Kellaway IW. In vitro peptide release from liquid crystalline buccal delivery systems. Int J Pharm 2000;195:29–33.
[11] Lara MG, Bentley MVLB, Collett JH. In vitro drug release mechanism and drug loading studies of cubic phase gels. Int J Pharm 2005;293:241–250.
[12] Komata Y, Kaneko A, Fujie T. Effect of fatty acid on the accumulation of thiamine disulfide in rat skin. Biol Pharm Bull 1994;17:705–708.
[13] Ogiso T, Iwaki M, Paku T. Effect of various enhancers on transdermal penetration of indomethacin and urea, and relationship between penetration parameters and enhancement factors. J Pharm Sci 1995;84:482–488.
[14] Bender J, Simonsson C, Smedh M, et al. Lipid cubic phases in topical drug delivery: visualization of skin distribution using two-photon microscopy. J Control Release 2008;129:163–169.
[15] Qiu H, Caffrey M. The phase diagram of the monoolein/water system: metastability and equilibrium aspects. Biomaterials 2000;21:223–234.